CALCULATION OF THE STATIC LONGITUDINAL STABILITY OF MULTI-ENGINE TRACTOR-PROPELLER-DRIVEN MONOPLANES

Thesis by

Warren Amster

California Institute of Technology

Pasadena, California

1947

ACKNOWLEDGEMENTS

This report was made possible by a Fellowship Grant from the CONSOLIDATED VULTEE AIRCRAFT CORPORATION San Diego, California

The Grant is part of the Scholarship and Fellowship Program for assisting students in technical colleges in conducting research while they are studying for engineering degrees

The author wishes to express his appreciation for assistance from Mr. K. E. Ward and Mr. Hugo Pruss of the Consolidated Vultee Aircraft Corporation and for technical advice from Mr. R. E. Bell of the California Institute of Technology.

TABLE OF CONTENTS

I SYNOPSIS

This report has three main purposes:

1. To establish an engineering computation procedure for predicting $C_{M_{(c.g.)}}$ as a function of C_L for a multi-engine monoplane of conventional configuration with tractor propellers mounted on and forward of the wing.

2. To recommend aircraft configurations which will minimize the destabilizing effect of power.

3. To provide a physical explanation for the effect of power on stability.

II INTRODUCTION

Some recent high performance propeller-driven aircraft have shown very marked effects of running propellers on static longitudinal stability. Reports from this country and from England, Germany and France mention the phenomenon. Although the effect varies considerably in magnitude among different aircraft, it is almost always destabilizing. There is a considerable body of literature reporting on wind-tunnel investigations into this and contributory phenomena. It is the purpose of this report to compile the available information that seems pertinent to the subject and arrange it into a simple computation procedure to predict stability of monoplane tractor-propeller-driven aircraft.

The data upon which this report is based were taken by a great many different investigators with greatly varying experimental equipment and techniques. Whenever possible the results of several investigators have been checked against each other in order to verify any theory which attempted to describe their experimental results. In general the data correlated quite well. In several cases some rather broad assumptions were necessary in order to obtain values for quantities which were necessary for computation purposes and which were either not mentioned in the literature or not measured by the investigators. An example is model propeller characteristics which were obtained largely from propeller charts which were not necessarily those for the propellers used in the tests. Errors introduced by such assumptions were minimized by averaging the results of as many different tests as possible.

The method of presentation is planned to help give a physical reason for separate effects and then combine all separate effects into a complete calculation procedure. In Sec. III the separate forces and

moments are discussed and means for calculating them presented. Sec. IV gives equations for combining all effects so that curves of C_L vs. α and C_M vs. C_L can be calculated for a complete airplane with power on.

In several reports cited as references, stability curves show characteristics for which the investigator who noted then had no explanation. These effects will be discussed in connection with the particular part of the calculations that they affect. They are seldom of primary importance but they sometimes have a noticable effect on stability and they can not be predicted by the calculations employed in this report. The complicated interaction and interference associated with flow of a slipstream over parts of an airplane could logically be expected to result in some uncalculable forces and moments. However these unexplained effects are definitely associated with particular aircraft and are shown not to be typical of any general configuration. It is assumed that they are the result of nacelle shape, fillets, spanwise flow, separation or some other arbitrary characteristic of particular aircraft. Wind tunnel tests appear to be the only way of predicting such effects.

Scope

Configuration: The calculation method of this report is applicable to the following type of aircraft:

1. A conventional monoplane with tractor propellers on nacelles mounted on the wing. The airplane may have any even number of propellers. The axis of propeller rotation must pass reasonably close to the wing chord line.

The following special cases may be treated by this analysis:

1. Unsymmetrical power.
2. All propellers turning in same direction.
3. Opposite rotating propellers with propeller blades moving up in the center.

4. Tailless aircraft with tractor propellers.

5. Any number of propellers feathered.

The following cases may not be treated by this method:

1. Extended flaps, spoilers, dive brakes, fuselage brakes, bomb bay doors, or landing gear and externally attached bombs, torpedoes, armament or fuel tanks whenever any of these objects interfere with the flow in the slipstream in such a way as to disturb the flow past the wing or tail of the airplane. Whether this disturbance will invalidate the analysis is left to the discretion of the designer.

Power Conditions: Three distinct power conditions will be considered.

1. Constant thrust wind-tunnel power-model polar. For this condition the RPM of the model propeller is held constant throughout the test range of angle of attack.

2. "Matched Power" wind-tunnel power model polar. The RPM of the model propellers is varied for constant blade setting so that T_c' of the model equals T_c' for the simulated full-scale airplane flying at equivalent C_L.

3. Full scale airplane in flight. The airplane is assumed to fly from stall to maximum level flight speed with constant power output and constant propeller RPM.

Power conditions 2. and 3. can theoretically be treated as equivalent for all phenomena dependent on T_c' if scale and compressibility effects are neglected. Although T_c' is the same for these two cases, the conditions of constant blade angle for the model and constant propeller RPM for the full scale airplane introduce differences in C_p and J. These differences are usually small as shown in Ref.(15). However under certain circumstances it might be necessary to consider the cases separately. For the purposes of this report power conditions 2. and 3. will be assumed to be equivalent except where

the differences are important in which case they will be specifically noted.

The effect of Reynolds Number and Mach Number on the phenomena described in this report is not known.

Only conditions of steady state flight will be considered.

Notation

Dimensions. Throughout this report all equations are adjusted to use data with the following dimensions:

Lengths	-	Feet
Areas	-	Square Feet
Velocities	-	Feet per Second
Forces	-	Pounds
Pressures	-	Pounds per Square Foot
Moments	-	Pound-feet
Power	-	Foot Pounds per Second
Angles	-	Radians
Rotational Speeds	-	Revolutions per Second

Coordinate System. Fig. (1) shows the conventions for dimensions and angles used in this report.

Dimensions denoted by $x_{(\ )}$, $y_{(\ )}$ and $z_{(\ )}$ refer to a Cartesian coordinate system with its origin at the center of gravity of the airplane. The positive $x_{(\ )}$ direction is aft in the direction of the wing zero-lift line. The positive $y_{(\ )}$ direction is up normal to the direction of the wing zero-lift line. All $z_{(\ )}$ dimensions are positive and are measured normal to the plane of symmetry. Subscripts identify dimensions. All dimensions shown in Fig. (1) are positive except x_p. Dimensions measured in other directions are given symbols other than $x_{(\ )}$, $y_{(\ )}$ and $z_{(\ )}$.

Vertical angles denoted by $i_{(\ )}$ are referred to the $x_{(\ )}$ axis. They are positive when they are as shown in Fig. (1). The angle of incidence, α, is the angle between the x axis and the direction of

relative wind, positive as shown. Horizontal angles denoted by $\theta_{(\ )}$ are measured with respect to the plane of symmetry and are positive as shown in Fig. (1). Subscripts identify angles.

Forces are referred to any direction in keeping with their physical nature. As an example; lift is positive up, referred to a direction normal to the relative wind; thrust is positive forward, referred to the thrust axis.

All pitching moments are taken about the center of gravity of the airplane.

The right-hand side of the airplane is to an observer's right when he is standing behind the tail of the airplane, facing toward it and the airplane is parked on its landing gear.

A propeller has a right-hand rotation when the upper blades are moving to the airplane's right.

Symbols

Symbol	Description	Reference
A	Propeller Coefficient.	Fig. (2)
A_p	Distance from Propeller Plane to Center of Gravity, measured parallel to thrust axis, positive for tractor propellers.	
$\mathcal{R}_e$	Effective Aspect Ratio of Wing, power-off.	
a	Radial Velocity in Slipstream	
a_o	Slope of Lift Curve for Wing Airfoil Section in Infinite Aspect Ratio Wing.	
a_t	Slope of Normal Force Coefficient Curve for Stabilizer.	$dCn_t/d\alpha$
B	Propeller Coefficient	Fig. (2)
B_p	Distance from Thrust Axis to Center of Gravity, measured normal to thrust axis, positive for thrust axis above C.G.	
b	Propeller Blade Chord at r = 0.7D/2	
C	Propeller Factor.	Equation (10)
C_D	Drag Coefficient for Complete Airplane, power-off.	$C_D = C_{D_{p_e}} + C_{D_i}$
C_{D_i}	Induced Drag Coefficient	$C_{D_i} = C_{L_o}^2/\pi\mathcal{R}_e$
$C_{D_{p_e}}$	Parasite Drag Coefficient for Complete Airplane, power-off.	
C_L	Lift Coefficient for Complete Airplane, power-on.	$C_L = 2L/\rho V_o^2 S$ Equation (19)
ΔC_L	Lift Coefficient Increment due to Slipstream over Wing.	Equation (12)
C_{L_o}	Lift Coefficient for Wing Alone, power-off.	
C_M	Pitching Moment of Complete Airplane, power-on.	$C_M = 2M/\rho V_o^2 Sc$ Equation (20)
C_{M_o}	C_M at $C_{L_o} = 0$, power-off.	

Symbol	Description	Reference
C_{N_t}	Normal Force Coefficient of Stabilizer.	$C_{N_t} = 2L_t/\rho V_o^2 S_t$ Equation (16)
C_p	Power Coefficient.	$C_p = P/\rho N^3 D$
C_T	Thrust Coefficient.	$C_T = T/\rho N^2 D$
c	Mean Aerodynamic Chord.	
D	Propeller Diameter.	
D_1	Slipstream Diameter at Wing Center of Pressure.	Equation (12)
E	Number of Propellers Operating.	
e	Elevator Deflection Angle, positive for trailing edge down.	
e_v	Slipstream Deflection Angle.	Equation (10)
F	Slipstream Deflection Factor	Equation (10)
f	dC_M/dC_L of fuselage and Nacelles, power-off.	
G	Fraction of Stabilizer Area in Slipstream.	Fig. (6)
H	Slipstream Rotation Factor.	Fig. (4)
h	Dimensionless Slipstream Coordinate.	Equation (14)
i_p	Angle between Thrust Axis and x Axis.	Fig. (1)
i_t	Angle between Stabilizer Zero-Lift Line at e = 0 and x Axis.	Fig. (1)
Δi_t	Change in Angle of Stabilizer Zero-Lift Line due to Elevator Deflection.	$\Delta i_t = eK$
J	Propeller Advance-Diameter Ratio.	$J = V_o/ND$
j	Chord of Wing in Vertical Plane through Thrust Axis.	
K	Elevator Effectiveness Factor.	$K = \Delta i_t/e$
k	Span of Wing in Slipstream	Equation (12)
L	Lift Force on Airplane power-on measured normal to relative wind.	
L_T	Normal Force on Stabilizer.	
M	Pitching Moment of Airplane, power-on, taken about center of gravity, positive when moment tends to raise nose of airplane.	

Symbol	Description	Reference
m	Distance from Center Line of Slipstream to Wing Lifting Line.	
N	Propeller Rotational Speed	
n	Number of Blades per Propeller	
P	Power per Engine.	
Q	Propeller Solidity at r = 0.7D/2.	Equation (4)
q	Local Dynamic Pressure.	$q = \rho V^2/2$
q_o	Dynamic Pressure of Relative Wind.	$q_o = \rho V_o^2/2$
R	Propeller Normal Force Coefficient.	Equation (4)
r	Radial Coordinate of Propeller.	
S	Wing Area.	
S_t	Stabilizer Area.	
s	Slipstream Velocity Factor.	Equation (8)
T	Thrust Force, positive foreward, parallel to thrust axis, for one propeller.	
T_c	Thrust Coefficient.	$T_c = T/\rho V_o^2 D^2$
T'_c	Thrust Coefficient.	$T'_c = 2T/\rho V_o^2 S$
U	Slipstream Factor.	Equation (15)
u	Slipstream Velocity Increase Factor.	Equation (7)
V	Local Air Velocity.	
V_o	Velocity of Aircraft.	
v	Dimensionless Slipstream Coordinate.	Equation (13)
W	Total Velocity behind Propeller.	
w	Angle of Downwash from Wing at Stabilizer, power-off.	Ref. (24)
x_p	Abscissa of Propeller Hub.	Fig. (1)
x_t	Abscissa of Stabilizer Center of Pressure.	Fig. (1)
x_w	Abscissa of Wing Center of Pressure.	Fig. (1)
y_p	Ordinate of Propeller Hub.	Fig. (1)
y_t	Ordinate of Stabilizer Center of Pressure.	Fig. (1)

Symbol	Description	Reference
y_w	Ordinate of Wing Center of Pressure.	Fig. (1)
z_p	Distance from Propeller Hub to Plane of Symmetry, measured normal to plane of symmetry, always positive.	Fig. (1)
z_t	Stabilizer Semispan.	Fig. (1)
α	Angle of Attack, measured between wing zero-lift line and relative wind, positive when the nose is raised.	
α_t	Effective Stabilizer angle of Attack.	Equation (15)
η_t	"Stabilizer Efficiency Factor," power-off.	$\eta_t = V^2/V_o^2$ at stabilizer
θ_p	Horizontal Angle between Thrust Axis and Plane of Symmetry, positive as shown in Fig. (1).	Fig. (1)
λ	Lift Increment Function.	Fig. (7)
ρ	Air Density, in slugs/cubic foot.	
ψ	Angle of Flow Rotation in Slipstream.	

III EFFECT OF POWER ON AIR LOADS ACTING ON AIRCRAFT.

General Remarks.

The most common means of representing static longitudinal stability is a plot of $C_{M_{(c.g.)}}$ vs. C_L for any desired power condition. Stability is then measured by $-dC_M/dC_L$. In the simple theory without power the plot of C_M vs. C_L is a straight line if the center of gravity of the airplane is on the chord line. For this theory $-dC_M/dC_L$ can be calculated without calculating C_M first. The stability can also be calculated for the case where the center of gravity is above or below the chord line. However this configuration introduces curvature into the C_M vs. C_L curve and the trim condition is important so that C_M must be calculated and then equated to zero.

The introduction of running propellers into the configuration has a great many effects on C_L, $dC_L/d\alpha$, C_M and dC_M/dC_L. These effects depend on such variables as J, T'_C, tail length, location of thrust axis, and propeller characteristics. By making some very approximate assumptions it is possible to calculate $-dC_M/dC_L$ for trim at a given power condition. However there are many conditions under which these assumptions lead to extremely erroneous results. For this reason it was decided to calculate C_M as a function of C_L, power, and elevator deflection and use the graphical slope of the C_M vs. C_L curve to obtain $-dC_M/dC_L$. This is the form in which wind tunnel data are obtained and the correlation of the calculated and wind tunnel data is then quite simple.

Propellers.

Thrust. For any stability calculations it will be assumed that a standard performance analysis has already been carried out for the airplane so that "power available" curves are at the disposal of the

designer. From the "power available" curves and the condition of steady flight it is quite simple to calculate curves of power and thrust coefficients and advance ratio as functions of C_L for each propeller.

The propeller thrust coefficient which is analogous to C_L for static equilibrium calculations is T_c'. Ref. (9), Vol. IV, states that the thrust of a propeller is not affected by small angles of pitch with respect to the relative wind. It will be assumed here that T_c' is not affected by any angle of pitch encountered in flight.

T_c' may be calculated as a function of C_L as follows:

① $$T_c' = \frac{2C_T D^2}{J^2 S}$$

② Lift Component of T_c': $= ET_c' \sin(\alpha + i_p)$

③ Pitching Moment Contribution of T_c': $= -\frac{ET_c'B_p}{c}$

Propeller Normal Force. A running propeller whose thrust axis is at an angle to the relative wind experiences a force in the plane of rotation. This force is a function of the angle of inclination, thrust loading, thrust grading and number of blades.

Ref. (29) gives a method of computing the force for three representative blade planforms. The same data are used in Ref. (22) with a slightly different method. It appears that the method of Ref. (29) is in somewhat better agreement with experiment and it is used here.

The propeller side force coefficient analagous to C_L for static equilibrium calculations is $R(\alpha + i_p)$.

R may be calculated as a function of C_L as follows:

④ $$R = \frac{(AQ + BC_T)}{10}\frac{D^2}{S} \qquad \text{where} \quad Q = \frac{nb}{0.7\pi D}$$

A and B from Fig. (2)

⑤ Lift Component of Propeller Normal Force:

$$= ER(\alpha + i_p)\cos(\alpha + i_p)$$

⑥ Moment Contribution of Propeller Normal Force:

$$= \frac{ER(\alpha + i_p)A_p}{c}$$

A propeller at an angle to the relative wind also experiences a destabilizing moment about the propeller hub. Ref. (15) states that it is insignificant when compared with other pitching moments of the airplane. It will be neglected in this report.

Flow in the Slipstream.

Velocity Increase. The momentum theory for propellers treats the propeller as a disc with a pressure difference across it. The resulting potential flow is a contracting region of increasing velocity downstream of the propeller. Theoretically the slipstream develops an asymptotic velocity which extends to infinity. Actually viscous mixing at the slipstream boundary converts this energy into heat. Wake surveys show that in the region of the airplane actual conditions approximate the theoretical quite closely. Again it is assumed that tilting of the propeller axis does not affect the thrust of the propeller.

The increase in velocity in the propeller slipstream is most usefully expressed as a function of the ratio of $V^2_{(slipstream)}$ to V^2_o. This ratio is also the ratio of the dynamic pressures, q/q_o, which is of the most fundamental importance here.

Dynamic pressure ratios in the slipstream are calculated as functions of C_L as follows:

⑦ Dynamic Pressure Ratio at Propeller Disc:

$$q/q_o = (1 + u)^2 \qquad \text{where} \quad u = \frac{1}{2}\left[-1 + \sqrt{1 + \frac{8T_c}{\pi}}\right]$$

⑧ Dynamic Pressure Ratio at Wing Center of Pressure:
Note: This expression is given in Ref. (25) and is used in this report only for equations obtained from that reference.

$$q/q_o = (1 + s)^2 \qquad \text{where} \quad s = u\left[1 + \frac{(x_w - x_p)}{\sqrt{\frac{D^2}{4} + (x_w - x_p)^2}}\right]$$

⑨ Dynamic Pressure Ratio at Stabilizer Center of Pressure:

$$q/q_o = (1 + 2u)^2 = 1 + \frac{8T_c}{\pi}$$

Deflection of Slipstream. A propeller with its thrust axis inclined to the relative wind experiences two forces normal to the relative wind both in the same direction. One force is the thrust component normal to the relative wind, the other force is the normal force in the propeller plane. These forces arise from a change of momentum of the air normal to the relative wind. The effect of this momentum change in the slipstream is a deflection toward the inclined thrust axis.

Ref. (9), Vol. IV, gives an expression for the ratio of the inclination of the slipstream to the inclination of the thrust axis for small angles of deflection. Experimental data in Refs. (5, 12, 17, 21, 26, 28) indicate that this expression gives sufficiently accurate results for all angles encountered in flight. The angle of inclination of the slipstream to the relative wind is $e_v = F(\alpha + i_p)$. This angle tends to decrease due to viscosity effects downstream of the propeller. The theoretical expression for this decrease given in Ref. (25) is complicated and of doubtful accuracy. The downstream decrease in angle will be expressed as an empirical correction factor for any condition where it is important. This factor is determined from experimental data.

e_v may be calculated as a function of C_L as follows:

⑩ $e_v = F(\alpha + i_p)$ where $F = \dfrac{2u(1+u)\left[1+(C/T_c)\right]}{(1+2u)\left\{1+u\left[1+(C/T_c)\right]\right\}}$

F is plotted as a function of T_c and C in Fig. (3). This plot should be used for design purposes.

$$u = \frac{1}{2}\left[-1 + \sqrt{1 + \frac{8T_c}{\pi}}\right]$$

$$C = \frac{RS}{2D^2}$$

R from Equation ④

Note: The expression in Ref. (9) uses values for C which are calculated differently than is done here. The physical significance of the two factors is the same and the one given here is used because it is simpler to calculate and seems to be more accurate.

Rotation in the Slipstream. The torque of a running propeller results in rotational velocity components of flow in the slipstream. The radial distribution of rotation immediately downstream of the propeller disc depends on the torque grading of the propeller. However in the vicinity of the stabilizer it was found that the effects of viscosity tend to give a characteristic shape to the rotational velocity distribution, the axial velocity distribution, and to the slipstream itself regardless of the original torque and thrust gradings.

In this report the method of finding the rotation in the slipstream is to derive a parameter upon which angle of rotation depends and then reduce experimental data to design curves in terms of that parameter. Data from Refs. (10, 11, 13, 17, 19, 21, 26, 27) were checked against the analysis given below and satisfactory agreement was found both for magnitude and distribution of the rotational angle.

Rotation in the slipstream is one of the flow phenomena which is not matched when a flying airplane with constant-speed propellers is

simulated in a wind tunnel by a model with fixed-pitch propellers. No data have been found which can give some indication of actual experimental variation for these cases. However the effect of these differences in slipstream rotation will be very small if the inboard propellers rotate in opposite directions and the power is symmetrical. For an airplane with the inboard propellers rotating in opposite directions or one inboard propeller feathered there will probably be some difference in the effect on stability of rotation in the slipstream for the full scale airplane and the "matched power" model wind tunnel test. Performing separate slipstream rotation calculations will show the magnitude of the difference and it is left to the discretion of the designer to decide whether it is so small as to be beyond the accuracy of the whole stability calculation.

Parameter Governing Slipstream Rotation as a function of C_L:

Ref. (9), Vol. IV gives (in the notation of this report):

$$dC_p/dr = \frac{4\pi^2 r^2 ua}{D^5 N^2}$$ where r = Radial coordinate of propeller.
u = Axial velocity increase factor.
a = Radial velocity in slipstream.

Ref. (9) also gives:

$$ua = \frac{1}{2} W^2 \sin 2\psi$$ where W = Resultant velocity behind propeller.
ψ = Angle of rotation in slipstream.

Substituting:

$$dC_p/dr = \frac{2\pi^2 W^2 (\sin 2\psi) r^2}{D^5 N^2}$$

By the mean value theorem W^2 and $\sin 2\psi$ can be replaced by mean values in front of the integral sign before integrating:

$$C_p = \frac{2\pi^2}{D^5 N^2} \int_0^R W^2 (\sin 2\psi) r^2 dr = \frac{2\pi^2 \overline{W^2} \overline{\sin 2\psi}}{D^5 N^2} \int_0^R r^2 dr = \frac{\pi^2 \overline{W^2} \overline{\sin 2\psi}}{12 D^2 N^2}$$

Assuming that ψ is small and using a mean value of the thrust loading:

$$\sin 2\psi \doteq 2\psi$$

$$\overline{w^2} = V_o^2\left(1 + \frac{8T_c}{\pi}\right) \qquad \text{Far downstream of the propeller.}$$

$$\overline{\psi} = \frac{6C_p N^2 D^2}{\pi^2\left(1 + \frac{8T_c}{\pi}\right)V_o^2}$$

$$\overline{\psi} = \frac{6C_p}{\pi^2 J^2\left(1 + \frac{8T_c}{\pi}\right)} \qquad (11)$$

This analysis indicates that the mean angle of rotation in the slipstream is a linear function of $C_p/\left[1 + (8T_c/\pi)\right] J^2$. Assuming a radial distribution of ψ at the stabilizer which was obtained experimentally permits calculations of ψ as a function of r and $C_p/\left[1 + (8T_c/\pi)\right] J^2$. The vertical component of ψ has the only primary effect on stability because it contributes to the downwash at the stabilizer. Fig. (4a) shows the values of the downwash angle contribution of ψ throughout the slipstream in the vicinity of the stabilizer for $C_p/\left[1 + (8T_c/\pi)\right] J^2 = 1$. The use of this development in predicting the total downwash angle to which the stabilizer is subjected will be presented under "Stabilizer Pitching Moment" on Page (22).

Flow Over Wing and Nacelle:

Lift Increment. The region of increased velocity over the wing behind a propeller results in an increase in lift over that portion of the wing. Spanwise and chordwise lift distribution surveys of Ref. (26) show that the rotational components of velocity in the slipstream have a first order effect on spanwise lift distribution. However the total lift increment can be calculated without regard to rotation provided the propeller is far enough ahead of the wing leading edge. This is the situation for the usual nacelle arrangement of modern aircraft.

The lift increment is calculated as ΔC_L and added to the lift of

the wing without slipstream. Ref. (25) gives a simple direct method of calculating the lift increment. In this method the circulation of the wing is assumed to be undisturbed in the vicinity of the slipstream and the lift increment comes from the increased velocity. This assumption seems to be a good approximation of actual conditions as verified both by force and downwash measurements.

ΔC_L due to power may be calculated as follows:

⑫ $$\Delta C_L = \frac{Ekjs}{S}(C_{L_o}\lambda - 0.6a_o e_v)$$

where s from Equation ⑧

e_v from Equation ⑫

$k = \sqrt{D_1^2 - 4m^2}$

$D_1 = D\sqrt{\frac{1+u}{1+s}}$

$m = (y_p - y_w) + (\alpha - e_v)(x_w - x_p)$

λ = 1 for two engine airplanes. See Fig. (8) for four and six engines.

Note: s, e_v and α are functions of C_L. However C_{L_o} appears in the expression C_L. The successive approximation method for finding C_L will be discussed on Page (27).

Other Effects. Experiments in Ref. (17, 21, 26, 28) indicate that the pitching moment increment of C_{M_o} due to a slipstream passing over a wing is negligible.

The flow near nacelles is of such a random nature that no calculation of its effects can be made. The usual procedure of estimating power-off nacelle contribution to pitching moment is all that can be recommended. Unfortunately pronounced interference effects can occur which are of some unknown nature. Ref. (1) cites several cases of noticeable effects on the pitching moment of different propeller rotation modes. The effects were noted in wind tunnel tests and no information on verification by

flight tests is available. No instance of any such interference on a wing without nacelles has been noted.

Flow Over Stabilizer.

The flow in the vicinity of the horizontal stabilizer of a conventional tractor multi-engine monoplane consists of a region of potential flow downwash surrounding well defined, characteristically shaped slipstreams. The distortion from a cylindrical shape of the slipstreams results from the interaction of the rotational components of the slipstream and the wing. In the region where the slipstream flows past the wing the vertical components of the rotation are blocked while the horizontal components cause horizontal translations of the upper and lower portions in opposite directions. Downstream of the wing these two sheared portions do not reunite but tend to progress downstream rotating slightly and giving a shape to the slipstream which is shown in Fig. (4b). Since the rotation in the slipstream causes the shearing it is to be expected that the shape of the slipstream is a function of the rotational components in it. This is verified at least qualitatively by all the data available. However for the sake of simplicity in computation an average shape will be used which is representative of wake survey data found in Ref. (6, 21, 26, 27). Attempts to calculate a more accurate shape for the slipstream lead to complications which do not appear to be justified because of a relatively minor increase in accuracy of the final calculations. Within the slipstream, the velocity distribution depends on the nacelle shape and size and on the thrust grading of the propeller. Data from Ref. (1, 6, 21, 27) show that for the purposes of calculation it is sufficiently accurate to assume that within the slipstream boundary the full theoretical velocity increment is developed and outside it the flow is that of an undisturbed wing wake.

Downwash at the stabilizer can be calculated accurately by the charts in Ref. (24). For such calculations the vertical position of the

stabilizer in the wing wake must be considered.

From finite wing theory w should be zero when $\alpha = 0$ because $C_{L_o} = 0$. Fuselage-wing interference sometimes causes a value of w as large as 2^o at $C_{L_o} = 0$. This "zero correction" for downwash with power off should be estimated from experience with similar fuselage-wing combinations or determined from wind-tunnel tests.

Location of the Slipstream. For the purposes of this report the following assumptions will be made in locating the center line of the slipstream at the stabilizer:

1. From the propeller disc to the wing center of pressure the slipstream is at an angle $0.75e_v$ with the relative wind. The factor 0.75 was obtained from analysis of experimental data found in Ref. (6, 13, 28). It is due to induced upwash at the propeller from the bound vorticity of the wing, viscous mixing at the slipstream boundary and the "inclined cylinder" effect described in Ref. (25).
2. Aft of the wing center of pressure the slipstream is inclined to the relative wind at the local downwash angle plus $0.75e_v$.
3. The downwash angle of the trailing vorticity of the wing varies from w/2 at the wing to w at the stabilizer and has a mean value of 0.75w.
4. The downwash angle in the slipstream is the same as it would be if the slipstream were not present. This is a result of the assumption of undisturbed circulation and is verified by experiments in Ref. (26).

Rather than find the location of the center of the slipstream directly, two much more useful coordinates defining this location will be used. These coordinates give the location of the tip of the stabilizer with respect to the center of the slipstream. Such coordinates, when made dimensionless by dividing by the propeller diameter, will

permit easy determination of the portion of the horizontal stabilizer which is in the slipstream. These dimensionless coordinates are v and h. v and h are calculated as functions of C_L as follows:

The distance below the propeller hub of the slipstream center at the wing center of pressure is:

$$(x_w - x_p)\tan(0.75e_v)$$

At the stabilizer center of pressure this distance is:

$$(x_w - x_p)\tan 0.75e_v + (x_t - x_w)\tan(0.75e_v + 0.75w)$$

The distance of the stabilizer below the propeller hub is:

$$(x_t - x_p)\tan\alpha - (y_t - y_p)$$

Subtracting and assuming all angles small so tangents can be represented by angles:

$$(x_w - x_p)0.75e_v + (x_t - x_w)(0.75e_v + 0.75w) - (x_t - x_p)\alpha + (y_t - y_p)$$

Collecting terms and dividing by D:

(13) $$v = \frac{(y_t - y_p) + (x_t - x_w)0.75w - (x_t - x_p)(\alpha - 0.75e_v)}{D}$$

Similiarly:

(14) $$h = \frac{(z_p - z_t) - F\theta_p(x_t - x_p)}{D}$$

where w = downwash angle at stabilizer in radians from Ref. (24), calculated from C_{L_o}.

e_v from Equation (10)

F from Equation (10)

Stabilizer Lift and Pitching Moment. A horizontal stabilizer in a propeller slipstream is subjected to a complex flow pattern which is further complicated by the presence upstream of a lifting wing. Across the span of the stabilizer both the velocity and the angle of attack vary. Furthermore the flow pattern changes as the angle of attack of

the airplane varies and the stabilizer moves through a vertical displacement. Calculation of the normal force coefficient of the stabilizer requires finding the spanwise flow pattern and then determining the force that such a flow pattern will produce.

In previous sections the nature of the flow near a stabilizer was discussed and a means of calculating it presented. The location of the center line of the slipstream is given by v and h. The next step is to combine the different flow regions experienced by the stabilizer into some equivalent uniform flow for calculation purposes.

The equivalent uniform flow experienced by the stabilizer will be described by an artificial parameter called "effective stabilizer angle of attack" and denoted by α_t. Actually α_t is the product of an average angle of attack and an average dynamic pressure ratio. The use of the idea of an "effective angle of attack" simplifies the calculation of the tail pitching moment. The calculation of α_t is based on the following assumptions:

1. Over the portion of the stabilizer outside the slipstream the downwash is w and the dynamic pressure ratio is η_t, which is the power-off "tail efficiency factor" and is either determined by experience or simply estimated. The normal force contribution of this portion of the stabilizer is proportional to its area.
2. Over the portion of the stabilizer inside the slipstream the downwash is $w + 0.75e_v$ plus rotational components. The dynamic pressure ratio is $\left[1 + (8T_c/\pi)\right]\eta_t$. The normal force contribution of this portion of the stabilizer is proportional to its area.
3. The rotational angle of downwash in the slipstream has the distribution shown in Fig. (4a) and a magnitude which is a linear function of $C_p/\left[1 + (8T_c/\pi)\right]J^2$. The "effective" angle

of rotation is obtained by multiplying the true angle by the dynamic pressure ratio which is $\left[1 + (8T_c/\pi)\right]\eta_t$ at the tail. Therefore the "effective" angle of rotation depends linearly on C_p/J^2. Fig. (5) gives curves for calculating the contribution to the total "effective stabilizer angle of attack" of rotational velocity components in the slipstream. This quantity is actually $\left[1 + (8T_c/\pi)\right]$ $(1/D)\int$ dr integrated over the portion of the stabilizer in the slipstream for $C_p/J^2 = 1$. It is called H and is obtained from v and h for a variety of propeller rotation modes as shown in Fig. (5). H must be multiplied by C_p/J^2 and $D/2z_t$ in order to obtain the increment of α_t with the proper dimensionless magnitude.

4. For calculation of stability with one inboard propeller feathered it is assumed that the dynamic pressure ratio at the stabilizer on the side of the airplane where the propeller is feathered is η_t. The downwash on that side is w. On the side where the engine is operating the assumptions are the same as above.

5. For moderately unsymmetrical power from the inboard engines it is assumed that both engines are operating at a T_c' which is a mean of their two values.

The use of an "effective stabilizer angle of attack" is suggested in Ref. (26) where it is called the "tail flow efficiency." Ref. (1) uses somewhat the same approach to investigate the effect on stability of propeller operation for five airplane models. However the calculations of Ref. (1) are based on a circular slipstream shape and no attempt was made to calculate the effect of rotational flow in the slipstream. Experimental data from Ref. (1, 6, 21, 28) are in quite good agreement with the theory presented here.

α_t, the "Effective Stabilizer Angle of Attack", is calculated as follows:

Outside the slipstream the contribution to the effective angle of attack is:

$$\eta_t(\alpha + i_t + Ke - w)(1 - G)$$ where G is the fraction of the stabilizer area in the slipstream.

Inside the slipstream the contribution is:

$$\eta_t \left(\alpha + i_t + Ke - w - 0.75e_v\right) \left[1 + (8T_c/\pi) G + \frac{DC_pH}{2z_tJ^2}\right]$$

Adding these together:

(15) $$\alpha_t = \eta_t\left[(\alpha + i_t + Ke - w)\left\{1 + (8GT_c/\pi)\right\} - 0.75e_vG\left\{1 + (8T_c/\pi)\right\} + \frac{DC_pH}{2z_tJ^2}\right]$$

where $T_c = \frac{C_T}{J^2}$

e_v from Equation (10)

w = downwash angle at stabilizer in radians from Ref. (24) calculated from C_{L_o}.

H from Fig. (5) using v from Equation (13) and h from Equation (14).

G the fraction of the stabilizer area immersed in the slipstream is obtained as follows:

1. Obtain U from Fig. (6) using v and h.
2. Obtain G from Fig. (7) using $DU/2z_t$ and the taper ratio of the stabilizer.

K = elevator effectiveness factor $\Delta i_t/e$.

e = elevator deflection.

The next consideration is the slope of the stabilizer normal force coefficient vs. angle of attack curve. No general theoretical method of predicting the characteristics of a stabilizer is available. Such reports as Ref. (14, 23) give the results of tests on existing

stabilizers. Data of this sort seems to be the best way to predict the slope of the stabilizer normal force coefficient curve and the elevator effectiveness. For the purposes of this report the characteristics of the stabilizer attached to the airplane fuselage, but with wing removed, will probably give best results. However Ref. (13) indicates that these characteristics do not vary greatly from those of the isolated stabilizer.

The use of an "effective stabilizer angle of attack" introduces a difficulty in using stabilizer characteristic curves. Since α_t has no real physical significance there is no way to predict at what angle the lift will start to level off and the stabilizer eventually stall. Curvature in the stabilizer normal force coefficient curve at comparatively low angles of attack would lead to particularly large inaccuracies. Since high elevator deflection often causes just such curvature, calculations involving high elevator deflections should be regarded as probably inaccurate. The effect of a slipstream on the stall characteristics of a stabilizer is not known.

Lift and Pitching Moment Contributions of the Stabilizer may be calculated as a function of C_L as follows:

⑯ $C_{N_t} = \alpha_t a_t$ where C_{N_t} = stabilizer normal force coefficient.

α_t from Equation ⑮

a_t = slope of stabilizer normal force coefficient vs. angle of attack in radians curve for fuselage and stabilizer only, or isolated stabilizer.

⑰ Lift Contribution of Stabilizer: $= \dfrac{C_{N_t} S_t}{S}$

⑱ Pitching Moment Contribution of Stabilizer: $= - \dfrac{C_{N_t} S_t x_t}{Sc}$

IV CALCULATION OF POWER-ON STABILITY

The following procedure is planned for tabular calculation. For most applications, curves of C_L vs. α and C_M vs. C_L will be desired for a series of flight power conditions at various elevator deflections. Since the C_M vs. C_L curve is not straight with power-on, the trim condition ($C_M = 0$) gives the only value of $(-dC_M/dC_L)$ which has a physical significance for steady state flight.

For stability calculations it is assumed that all physical dimensions of the airplane are known and power-off aerodynamic characteristics are known or estimated. Power conditions must be specified. From the standard "power available" curves and the condition of steady state flight it is possible to calculate T_c' as a function of C_L. The following power conditions may be assumed in the stability calculations.

1. "Constant thrust" power-model wind-tunnel test. For this case J, C_p and T_c' are constant throughout the range of C_L of the test.
2. "Matched Power" model wind tunnel tests. T_c' varies with C_L in exactly the same manner as in the case of the full scale airplane. C_p and J are calculated as functions of C_L for constant blade angle of model propellers.
3. Full scale Airplane. In this case C_p is constant assuming constant power, propeller speed and altitude. T_c' and J are functions of C_L.

These power conditions are discussed in greater detail under Scope on Page (4).

C_L vs. α Curve.

In computing the total lift coefficient for a chosen angle of attack, the direct porpeller forces and the lift increment due to the slipstream passing over the wing are added to the lift coefficient

for the wing with power-off. This procedure makes the calculation of C_L as a function of α a successive approximation process but finding C_M as a function of C_L is a direct calculation. Consideration of the lift of the stabilizer in finding C_L makes the computation of C_M as a function of C_L a successive approximation process also and it is not normally recommended. In this report the lift of the stabilizer will not be used in computing C_L.

C_L for a chosen value of α may be calculated as follows:

⑲ $$C_L = C_{L_o} + \Delta C_L + T'_c(\alpha + i_p) + R(\alpha + i_p)\cos(\alpha + i_p)$$

1. Find C_{L_o} for the chosen value of α from finite wing theory. It should be remembered that α is referred to the zero lift line.
2. Estimate the value of C_L.
3. Find T'_c, T_c, C_T, and J for the estimated C_L.
4. Find R from Equation ④ and Fig. (2) using J, C_T, and the propeller blade planform.
5. Calculate e_v from Equation ⑩ using Fig. (3) and R, T_c, and α.
6. Calculate ΔC_L from Equation ⑫.
7. Calculate C_L from Equation ⑲ using C_{L_o}, ΔC_L, T'_c, R and α as obtained above.
8. If C_L as calculated agrees with the estimated C_L from step 2., then it is a correct value. If it does not agree use the calculated value as a second approximation and repeat until closure. This process will usually converge very rapidly.
9. Repeat procedure for other values of α.

C_M vs. C_L Curve.

Once the C_L vs. α curve has been established for a specified power condition, the determination of C_M as a function of C_L is a direct calculation. It is a considerable simplification here to choose

values of C_L which were determined by the previous calculations in order to use values of variables which have already been calculated.

C_M for a chosen value of C_L may be calculated as follows:

(20) $$C_M = C_{M_o} + \left[f - \frac{(x_w \cos\alpha + y_w \sin\alpha)}{c}\right](C_{L_o} + \Delta C_L) + \frac{(y_w \cos\alpha - x_w \sin\alpha)}{c} C_D - \frac{ET'_c B_p}{c} + \frac{ER(\alpha + i_p)A_p}{c} - C_{N_t} \frac{S_t}{S} \frac{x_t}{c}$$

1. C_L, C_{L_o}, ΔC_L, α, T'_c, T_c, C_p, J and e_v are known from calculating C_L as a function of α or are determined the same way.
2. C_{M_o} is estimated for the airplane without power.
3. f is the increment of dC_M/dC_L due to fuselage and nacelles without power.
4. $C_D = C_{D_{p_e}} + C_{D_i}$ for the entire airplane without power and is assumed to act through the wing center of pressure. $C_{D_i} = C_{L_o}^2 / \pi A_e$.
5. Calculate w in radians at the stabilizer from charts in Ref. (24). Use C_{L_o} to calculate w.
6. Calculate v and h from Equation (13) and (14).
7. Find H from Fig. (5) using v and h.
8. Find U from Fig. (6) using v and h.
9. Find G from Fig. (7) using $DU/2z_t$ and the taper ratio of the stabilizer.
10. Determine a_t and K from Ref. (14, 23) or other references or from tests.
11. Calculate α_t from Equation (15) using α, w, T_c, G, e_v, C, J and H.
12. Calculate C_{N_t} from Equation (16) using α_t and a_t.
13. Calculate C_M from Equation (20).

14. Repeat for other values of C_L with the same power setting and elevator deflection. This will give a curve which may be faired and $(- dC_M/dC_L)$ obtained graphically.
15. Repeat process for other elevator deflection. The value of α_t is the only variable affected by elevator deflection.
16. Repeat process for other power settings. A new C_L vs. curve must be calculated for each new power setting.

Things to check before making any calculations:

1. Be sure that all length dimensions have the proper sign as determined by the coordinate system.
2. Be sure that all angles are in radians.
3. Be sure that the slopes of the lift and normal force coefficient curves are for angle of attack in radians.
4. Be sure that C_p and T_c' are calculated for the power from one engine.
5. Be sure that the flaps are retracted.

V DESIRABLE CONFIGURATION FOR POWER-ON STABILITY

The undesirable effects of power-on static longitudinal stability usually appear most pronounced at high lift coefficients. This phenomenon has two basic reasons. First, the thrust coefficients which describe the propeller effects on stability increase with increased C_L. Second, the angle between the propeller axis and the relative wind increases with increased C_L. The direction of inboard propeller rotation also has a pronounced effect on stability because of flow at the stabilizer.

The following recommendations will usually improve static longitudinal stability at high lift coefficients:

1. The thrust axis should be inclined downward so that it is parallel to the relative wind at as high a lift coefficient as possible. This does not decrease the lift coefficient at lower angles of attack due to the downward component of the thrust as might be expected. Experiments in Ref. (26) show that the effect of the increased local angle of attack in the slipstream almost exactly balances the downward thrust component giving a constant C_L over a wide range of thrust axis inclination. This improvement is limited by the possibility of local stalling of the wing behind the propeller blades which are moving upward or early separation in the same region with laminarflow airfoils.
2. The most desirable propeller rotation mode is with the inboard propellers rotating in opposite directions and the in board blades moving upward. This configuration causes the rotation in the slipstream to improve stability for aircraft where the stabilizer span is about the same as the distance between the inboard propeller hubs. There is often a slight increase in C_L with this rotation mode because of

a better spanwise lift distribution over the wing in the region of the fuselage. The case of both inboard propellers rotating in the same direction usually has very little effect on stability from rotational flow in the slipstream. Co-axial counter-rotating propellers presumably have no rotational components of flow in the slipstream although this case was not investigated and no experimental data are included among the references cited this report. Opposite-rotating inboard propellers with the inboard blades moving downward have a very destabilizing effect and it is recommended that they not be used for aircraft of the general configuration considered in this report. For tailless aircraft the direction of propeller rotation would presumably not have any affect on static longitudinal stability except perhaps the interference effect with the nacelles which is not subject to prediction by numerical calculation methods.

3. The stabilizer should be located as low as possible in an effort to place it below the slipstream at high lift coefficients. This is more easily accomplished if the thrust axis is inclined downward. The region below the slipstream has an appreciably smaller angle of downwash than that above it where the wing wake is most pronounced and the velocity is decreased by flow over the wing. Ref. (6) gives the results of tests on a twin-engine model with the stabilizer in three vertical positions and the low position yields the best stability. Wake surveys in Ref. (13, 21, 26) show the same results. It should be mentioned in the interest of objectivity that Ref. (3) gives the results of tests on a single-engine low-wing monoplane with the stabilizer in three vertical positions and the highest position gives best

stability. Possibly the flow near the fuselage would invalidate this result as it concerns multi-engine aircraft. There is some indication that a low stabilizer position is undesirable for the flaps deflected configuration due to the change in the zero lift line and the wing wake position. The wake surveys which show the flow behind flapped wings are so confusing that no general conclusions can be drawn. The limitation in lowering the stabilizer is the possibility of buffeting from the wing wake or exciting natural vibration modes by oscillating velocity components in the slipstream at high speeds.

VI DISCUSSION AND RECOMMENDATIONS.

In order to evaluate the usefulness of the procedure presented in this report it would be necessary to carry out the calculations for applicable aircraft whose power-on stability characteristics are known. This was not done because of lack of time for completing the report and because it was felt that the theory should be checked with data which were not used in its development.

Because the calculation procedure consists of adding together several increments of lift or moment coefficient in order to obtain a final value, it is possible to evaluate the probable accuracy of each step and so predict the probable source of any inaccuracies.

Probable Accuracy of C_L Calculation. The accuracy of the calculation of C_L depends largely on the accuracy of C_{L_o}. Such effects as fuselage-wing interference and fuselage lift would lead to inaccuracies in C_{L_o} if no corrections are used. The thrust component of propellers in a lifting direction could be somewhat inaccurate due to the effect of parts of the airplane on propulsive efficiency. The method of calculating C_L has been checked by a great deal of experimental data and appears to be entirely reliable for two engine airplanes and usually accurate for four and six engines. Neglecting the lift of the stabilizer leads to errors in the original computation for C_L but the amount of the error can be determined further on in the computation procedure when C_{N_t} is evaluated. In general it is felt that the calculation of C_L is well within the usual accuracy which can be expected of preliminary aerodynamic computations.

Probable Accuracy of C_M Calculations. Unfortunately the pitching moment coefficient is sometimes subject to several unpredictable effects which can arise from wing-nacelle, propeller-naceller and wing-fuselage

interference usually are associated with specific aircraft and no general means of predicting them is available. Any discussion of the accuracy of the computation of C_M suggested in this report will be confined to evaluations of individual contributions to C_M. If no unpredicted interference effects occur the discussion will then be applicable to the method as a whole.

Contributions to C_M from lift and drag forces on the wing and fuselage, direct propeller thrust and C_{M_o} are calculated by standard methods so no special comment is necessary. The method of calculating the force in the plane of propellers agrees with the limited experimental data available to verify it. The normal force on the stabilizer, C_{N_t}, represents the most questionable quantity in the moment coefficient calculation. The accuracy of the calculation of C_{N_t} depends directly on the accuracy with which the "effective stabilizer angle of attack" represents the effective flow at the stabilizer. There is considerable experimental verification of the angle for zero stabilizer lift in this effective flow. Available experimental data verify calculated values for $_t$ quite well but the method cannot be regarded as dependable without further checks. Determination of a value for a_t for a particular stabilizer-fuselage combination is often difficult so that exact verification of the usefulness of the concept of an "effective stabilizer angle of attack" is hard to obtain. Pending further experimental checks, the calculation of the stabilizer-pitching moment coefficient should be regarded only as a suggested procedure.

REFERENCES

1. Bell, R.W. and Storms, H.A., Jr.; GALCIT Thesis, 1941
   Some Aspects of the Effects of Propeller Operation on the Static Longitudinal Stability of an Airplane.

2. Belsley, S.E.; GALCIT Thesis, 1940
   The Determination of Two Parameters Dealing with Power-On Stability for a Model with Right-Hand Propellers.

3. Bolster, C.M.; J. Ae. S., Vol. 4, No. 10, August 1937
   Effect of Slipstream on Longitudinal Stability of a Low Wing Monoplane.

4. Bradfield, F.B.; R. and M., No. 1212, November 1928
   Preliminary Tests on the Effect on the Lift of a wing of the Position of the Airscrew Relative to it.

5. Bradfield, F.B.; R. and M., No. 1488, June 1932
   Wind Tunnel Data on the Effect of Slipstream on the Downwash and Velocity at the Tailplane.

6. Bryant, L.W. and McMillan, G.A.; A.R.C., No. 3603, June 1938
   The Longitudinal Stability of a Twin-Engined Monoplane with Airscrews Running.

7. Bryant, L.W. and McMillan, G.A.; A.R.C., No. 3744, October 1938
   Further Analysis of the Experiments on Longitudinal Stability of a Twin-Engined Monoplane with Airsrews Running.

8. Donlan, C.J.; N.A.C.A. A.R.R., November 1942
   Some Theoretical Considerations of Longitudinal Stability in Power-On Flight with special reference to Wind-Tunnel Testing.

9. Durand, W.F.; January 1934
   Aerodynamic Theory.

10. de Feriet, J.K. and Fauquet, A.; G.R.A. N.T., No. 2, March 1939
    Influence of Slipstream on Aerodynamic Characteristics of a Powered Model.

11. de Feriet, J.K. and Fauquet, A.; G.R.A. N.T., No. 4, May 1939
    Influence of Slipstream on the Aerodynamic Characteristics of a Powered Model.

12. Goett, H.J. and Pass, H.R.; N.A.C.A. Report, May 1941
    Effects of Propeller Operation on Pitching Moments of Single-Engine Monoplanes.

13. Katzoff, S.; N.A.C.A. Report, No. 690, 1940
    Longitudinal Stability and Control with Special Reference to Slipstream Effects.

14. Martinov, A. and Kolosov, E.; N.A.C.A. T.M., No. 941, May 1940
    Some Data on the Static Longitudinal Stability and Control of Airplanes. (Design of Control Surfaces)

15. Millikan, C.B.; J. Ae. S. Vol. 7, No. 3, January 1940
The Influence of Running Propellers on Airplane Characteristics.

16. Millikan, C.B., Russell, J.S. and McCoy, H.M.; J. Ae. S. Vol. 3 No. 3, 1936
Wind-Tunnel Tests on a High Wing Monoplane.

17. Muttray, H.; N.A.C.A. T.M., No. 876, September 1938
Investigations on Downwash Behind a Tapered Wing with Fuselage and Propeller.

18. Priestly. E.; R.A.E. Aero. No. 1944, May 1944
A Suggested General Method of Treatment of Static Longitudinal Stability with Propellers: Analysis of Full Throttle Model Data for Single-Engined Aircraft.

19. Ried, E.G.; N.A.C.A. T.N., No. 1040, July 1946
Wake Studies of Eight Model Propellers.

20. Ribner, H.S.; N.A.C.A. A.C.R., December 1943
Propellers in Yaw.

21. Rogallo, F.M. and Swanson, R.S.; N.A.C.A. A.R.R., January 1943
Wind-Tunnel Tests of a Twin-Engine Model to Determine the Effect of Direction of Propeller Rotation on the Static Stability Characteristics.

22. Rumph, L.B., White, R.J. and Grumman, H.R.; J. Ae. S. Vol. 9, No. 12, October 1942
Propeller Forces Due to Yaw and Their Effect on Airplane Stability.

23. Silverstein, A. and Katzoff, S.; N.A.C.A. Report No. 688, 1940
Aerodynamic Characteristics of Tail Surfaces.

24. Silverstein, A. and Katzoff, S.; N.A.C.A. Report No. 648, 1939
Design Charts for Predicting Downwash Angles and Wake Characteristics Behind Plain and Flapped Wings.

25. Smelt, R. and Davies, H.; R. and M., No. 1788, 1937
Estimation of Increase in Lift Due to Slipstream.

26. Stuper, J.; N.A.C.A. T.M., No. 874, August 1938
Effect of Propeller Slipstream on Wing and Tail.

27. Sweberg, H.H.; N.A.C.A. A.R.R., August 1942
The Effect of Propeller Operation on Air Flow in the Region of the Tail Plane for a twin-Engine Tractor Monoplane.

28. Sweberg, H.H.; N.A.C.A. A.R.R., November 1942
Full Scale Tunnel Investigation of the Control and Stability of a Twin-Engine Monoplane with Propellers Operating.

29. Hufton, P.A.; R.A.E. T.N. Aero. 1119, January 1943
Propeller Forces Due to Yaw and Their Effect on Airplane Stability.

TABLE OF FIGURES

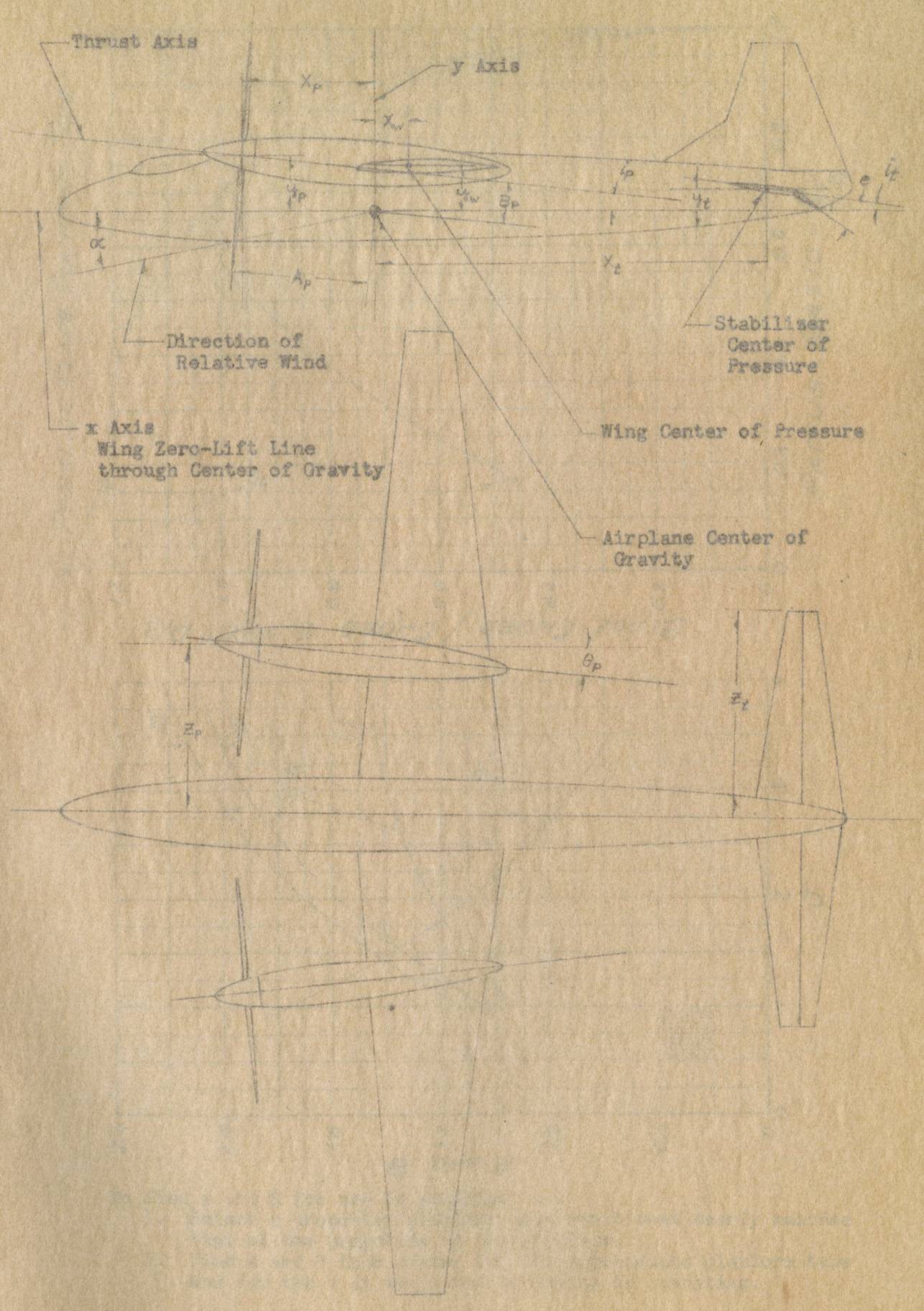

Fig. 1. Drawing Showing Dimensions and Angles.

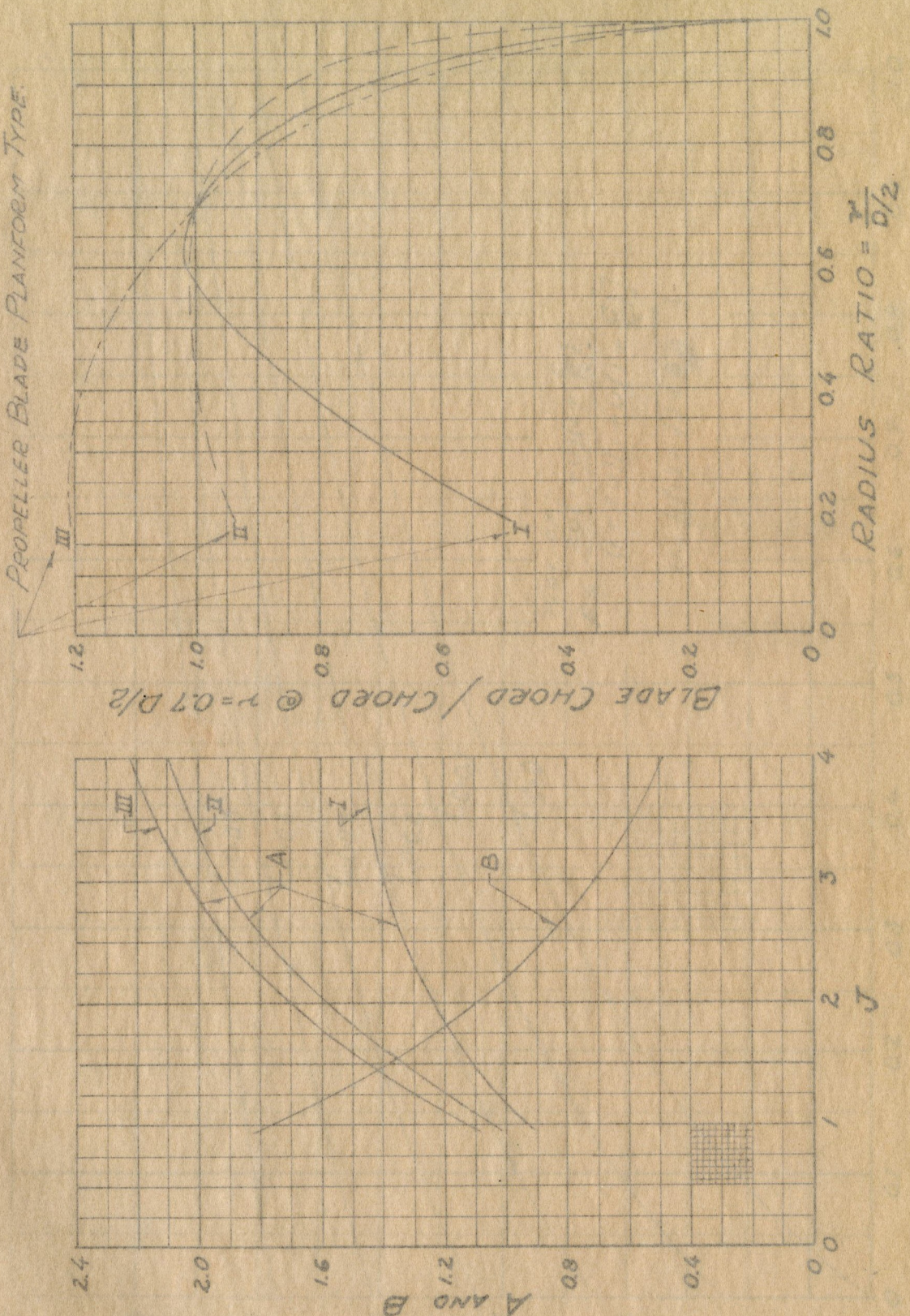

To find A and B for use in Equation 4 :

1. Select a propeller planform type which most nearly matches that of the propeller on the airplane.
2. Find A and B from curves for the appropriate planform type and for the J at which the propeller is operating.

Fig. 2. A and B as Functions of J and Propeller Planform.

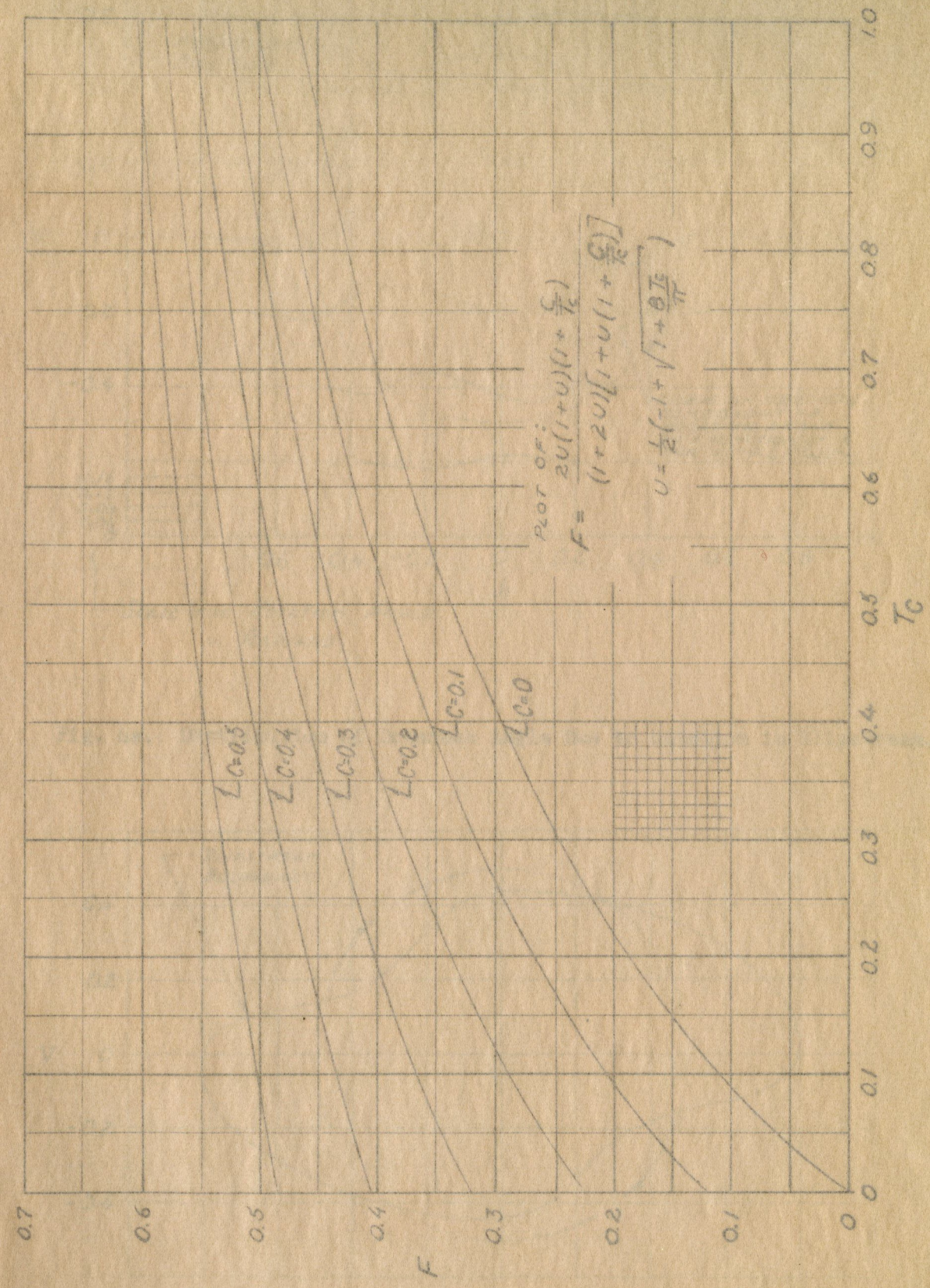

Fig. 3. F as a Function of T_c and C.

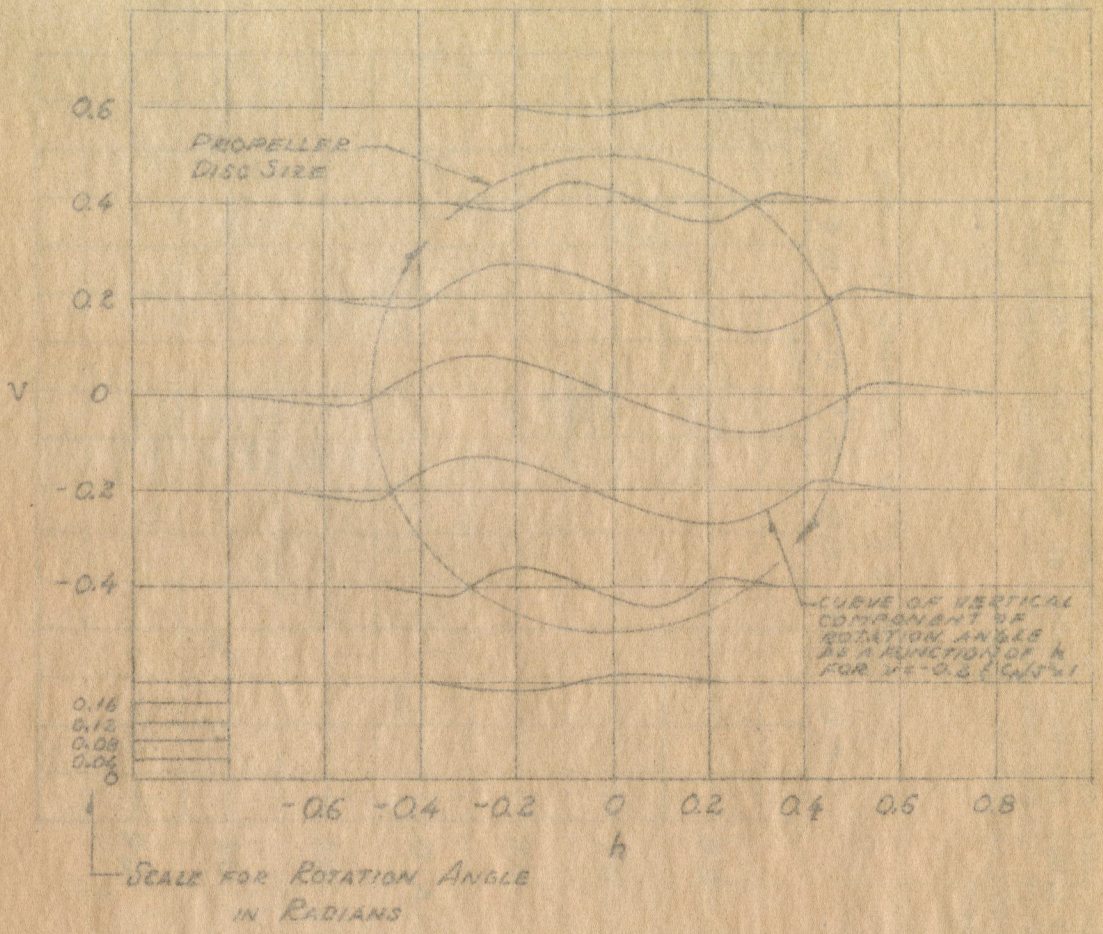

Fig. 4a. Distribution of Downwash Angle Due to Rotation in Slipstream.

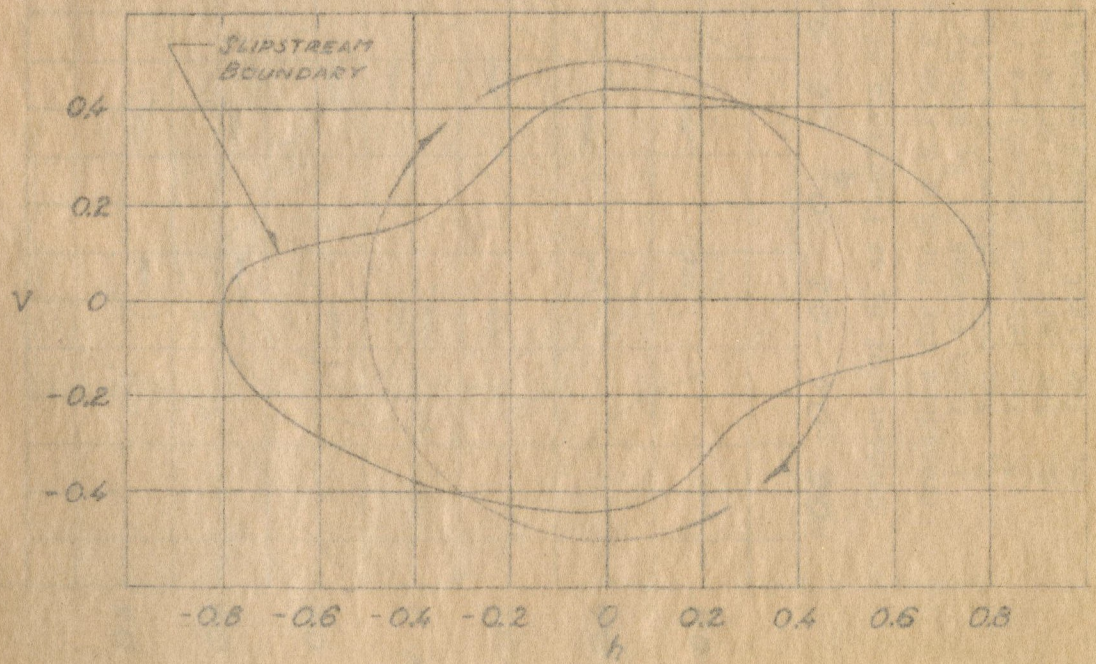

Fig. 4b. Shape of Slipstream at Stabilizer.

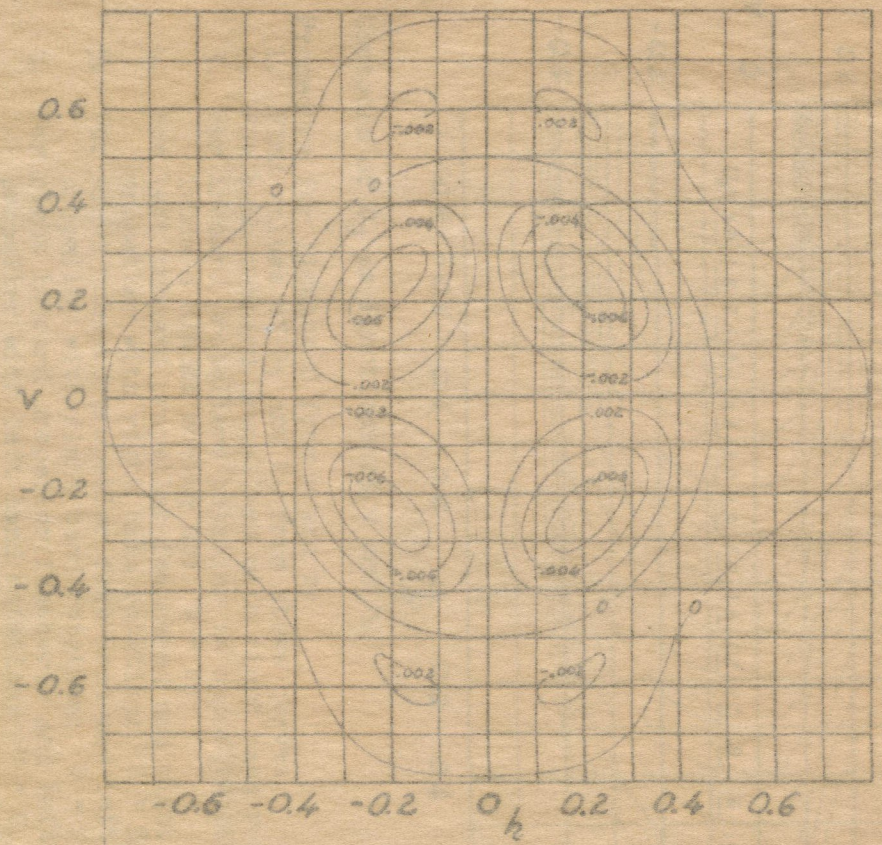

Contours of H_1 as Functions of v and h.

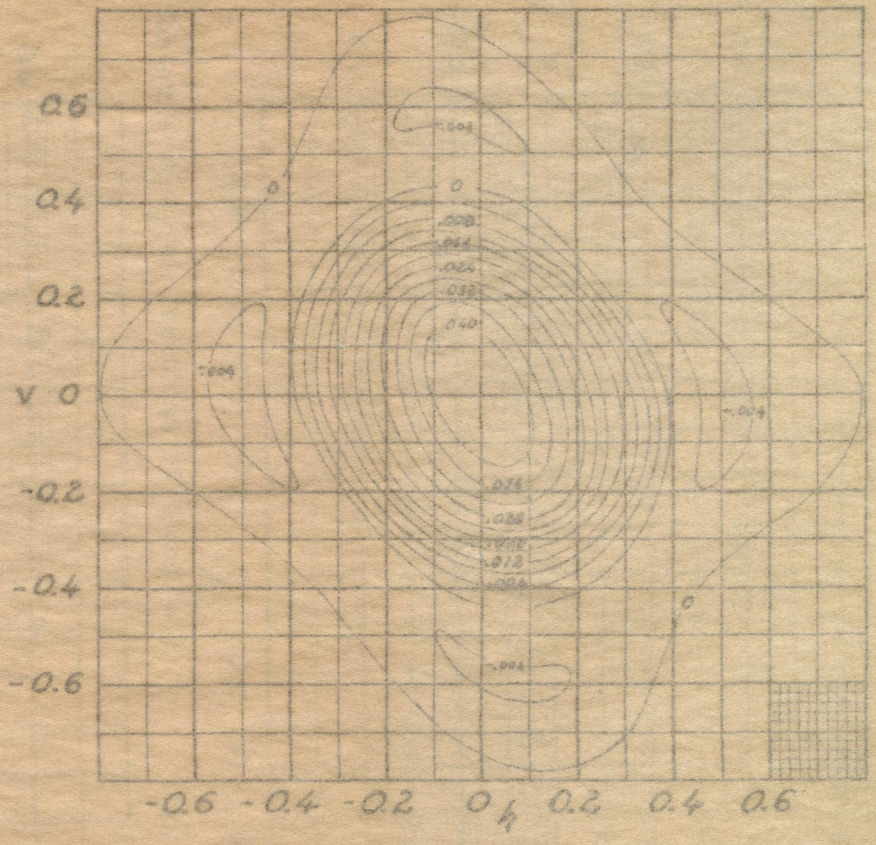

Contours of H_2 as Functions of v and h.

Procedure for finding H from v and h:

1. Find values of H_1 and H_2 from above curves.
2. For both inboard propellers with right hand rotation: $H = H_1$
3. For inboard propellers rotating in opposite directions and inboard blades moving up: $H = H_2$
4. For left inboard propeller feathered and right inboard propeller with right hand rotation: $H = H_2/2$
5. For right inboard propeller feathered and left inboard propeller with right hand rotation: $H = H_1 - H_2/2$
6. For right inboard propeller feathered and left inboard propeller with left hand rotation: $H = H_2/2$

Fig. 5. Curves and Procedure for Finding H as a Function of v and h.

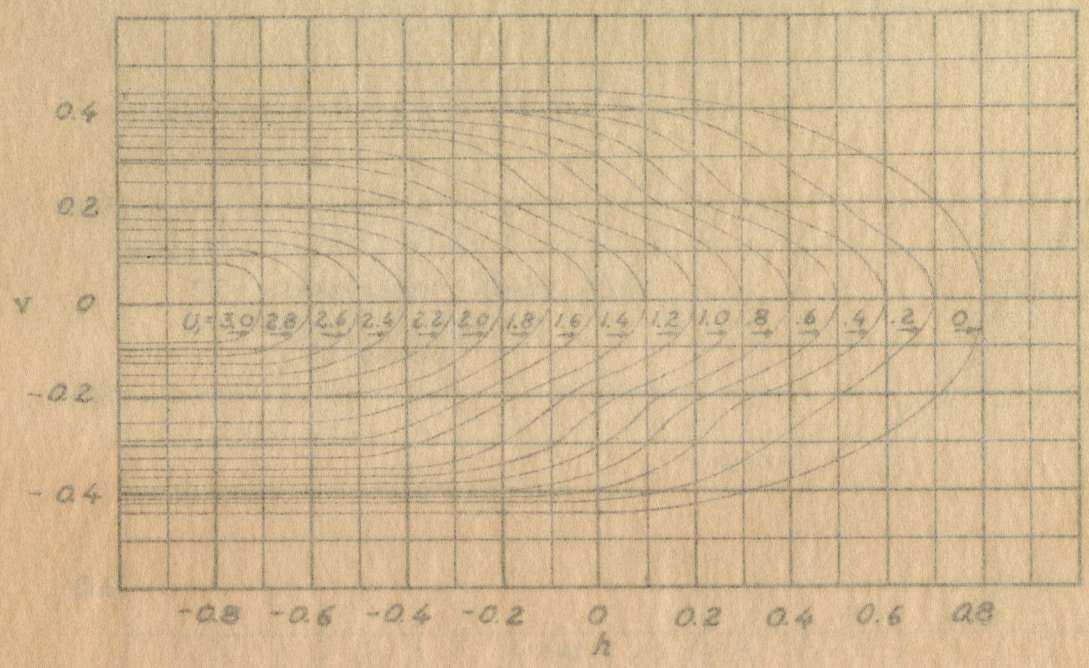

Contours of U_1 as Functions of v and h.

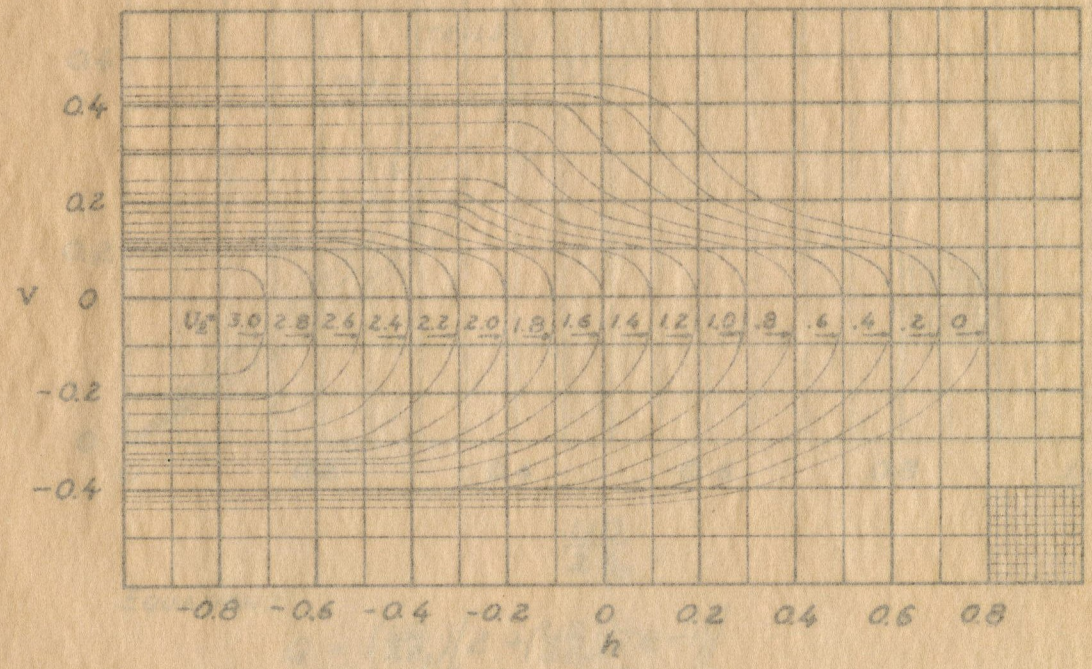

Contours of U_2 as Functions of v and h.

Procedure for finding U from v and h:

1. Find values of U_1 and U_2 from above curves.
2. For both inboard propellers with right hand rotation: $U = U_1$
3. For inboard propellers rotating in opposite directions and inboard blades moving up: $U = U_2$
4. For left inboard propeller feathered and right inboard propeller with right hand rotation: $U = U_2/2$
5. For right inboard propeller feathered and left inboard propeller with right hand rotation: $U = U_1 - U_2/2$
6. For right inboard propeller feathered and left inboard propeller with left hand rotation: $U = U_2/2$

Fig. 6. Curves and Procedure for Finding U as a Function of v and h.

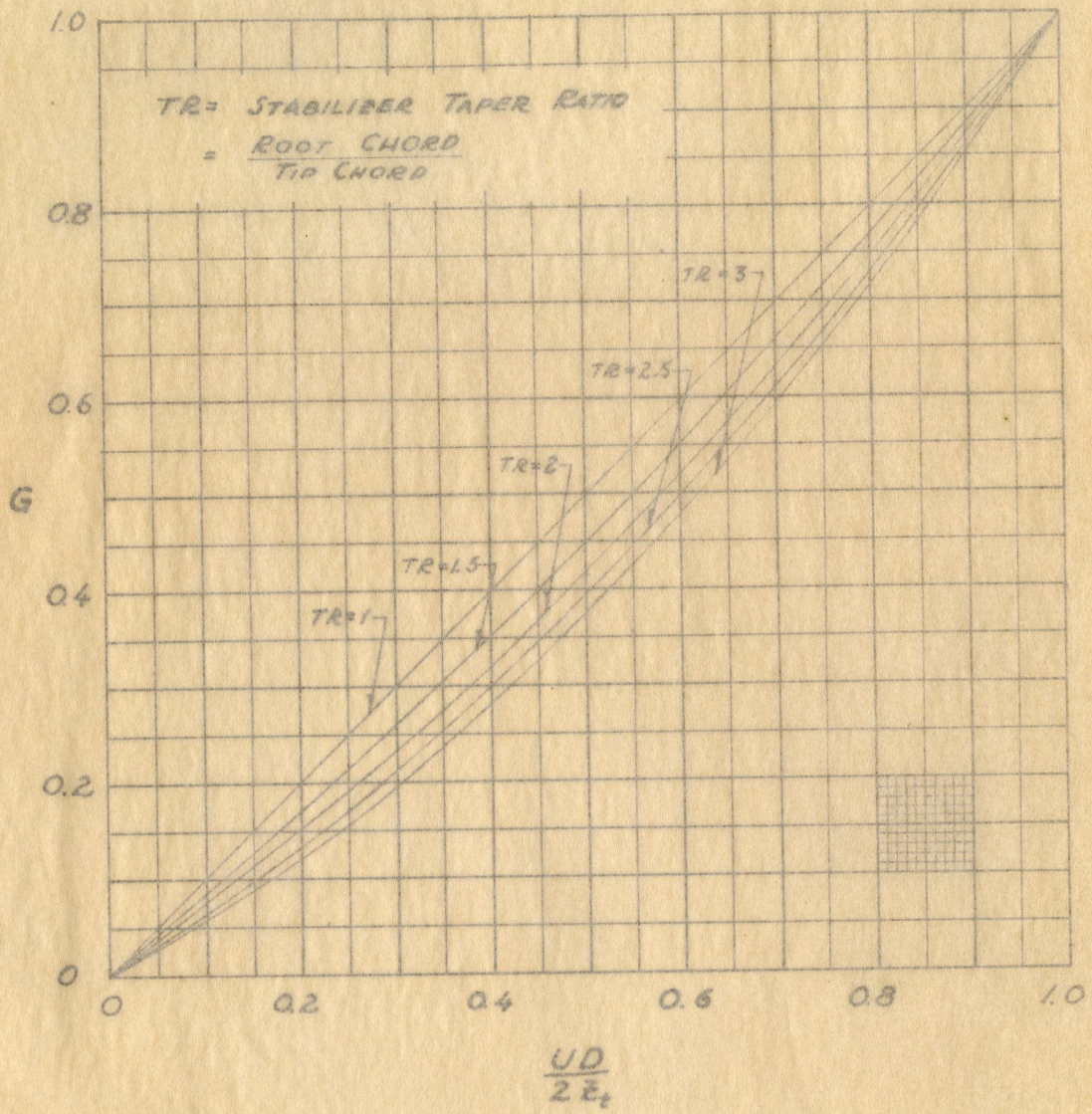

EQUATION:

$$G = \frac{\left(\frac{UD}{2\bar{z}_t}\right)\left[2 + \left(\frac{UD}{2\bar{z}_t}\right)(TR-1)\right]}{(TR+1)}$$

Fig. 7. Curves of G as a Function of U and Stabilizer Taper Ratio.

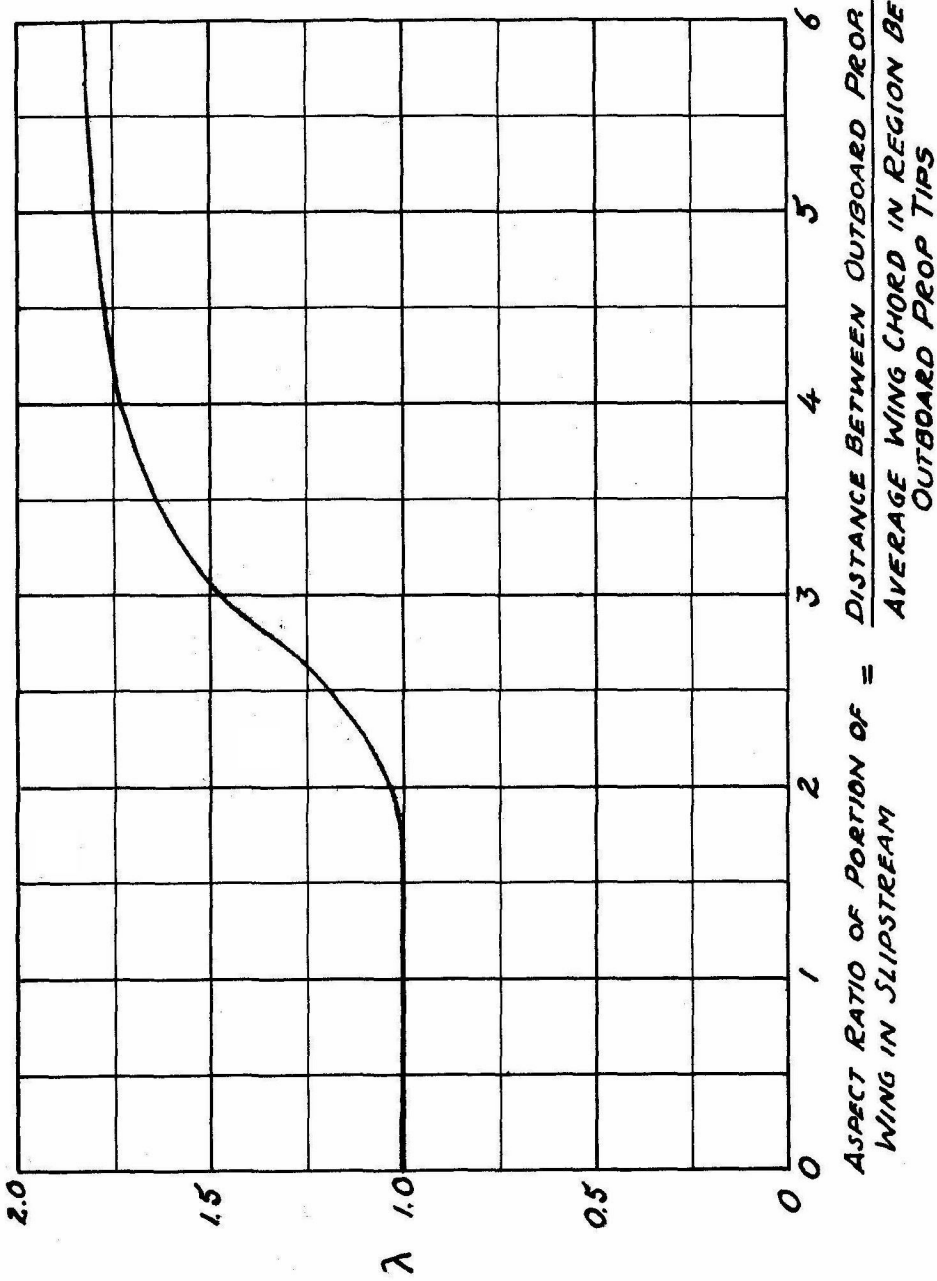

Fig. 8. λ as a Function of the Portion of the Wing in the Slipstream.